CXCR2 deficiency with myelokathexis caused by a novel variant: correction via CRISPR/Cas9

Myelokathexis is a severe form of neutropenia caused by retention of neutrophils in the bone marrow, with accumulation of both live and apoptotic neutrophils, resulting in neutropenia in peripheral blood.[1,2] One cause of myelokathexis is WHIM syndrome, a rare inborn error of immunity (IEI) named after its characteristics, including human Pappilomavirus-induced Warts, hypogammaglobulinemia, recurrent infections and myelokathexis.[3,4] More recently biallelic loss-of-function variants in *CXCR2* were reported to represent another WHIM-like IEI with neutropenia and varying degrees of myelokathexis.[5-7] CXCR2 deficiency is exceedingly rare with currently nine cases published.[5-7] The neutropenia characteristic of WHIM syndrome and CXCR2 deficiency stems from the essential roles of CXCR4 and CXCR2 in inhibiting and promoting neutrophil egress from the bone marrow into the blood stream, respectively. Stimulation of CXCR4 by its ligand C-X-C motif ligand 12 (CXCL12), which is constitutively expressed by bone marrow stromal cells, promotes neutrophil retention, whereas CXCR2 stimulation by interleukin 8 (IL-8) promotes release of neutrophils from the bone marrow to peripheral blood.[8,9] CXCR2, also known as interleukin 8 receptor β, is a G-protein-coupled seven transmembrane receptor for the CXC subclass of chemokines[10] expressed predominantly on neutrophils, and to a lesser extent on monocytes, macrophages, NK cells, and endothelial cells.[11,12]

Two brothers from a family of healthy non-consanguineous Norwegian parents and one healthy brother presented with severe neutropenia. Patient 1 (P1) had been suffering from frequent upper respiratory tract infections since the age of 1. He was diagnosed with neutropenia at 3 years of age at which time a bone marrow biopsy showed high cellularity (80% of cells being granulocytes) and myelokathexis. Immunophenotyping of peripheral blood mononucelar cells (PBMC) showed normal distribution of T, B, and NK cells with marginally increased fraction of plasmablasts. At age 29, he still experiences frequent tonsillitis/pharyngitis and suffers from severe gingival ulcerations. His neutrophil count has continuously been decreased in the range of 0.5-1.2x10^9/L (normal range 1.8-6.9x10^9/L) (Figure 1A; *Online Supplementary Figure S1A, B*). P2, the younger brother of P1, was admitted to hospital with pneumonia at the age of 3 years and was diagnosed with neutropenia at the age of 16, at which time hematological evaluation revealed persistent neutropenia. A bone marrow biopsy showed increased myelopoiesis and myelokathexis (estimated to affect ~33% mature granulocytes), with normal maturation of neutrophils, reminiscent of previous descriptions of myelokathexis in conjunction with WHIM syndrome (Figure 1B). During follow-up, the patient's neutrophil count has repeatedly been in the range of 0.1-0.2x10^9/L (*Online Supplementary Figure S1C*). At age 23 his major symptoms are ulcerations in the nose and oral cavity. Both parents and a third younger brother were healthy without oral ulcerations or infections (although the mother experienced 1 episode of neutropenia) and with neutrophil counts in the lower normal range (father 2.1x10^9/L, mother 2.8x10^9/L and brother 3.2x10^9/L). The patients, their family, and healthy controls were included following oral and written consent in accordance with Declaration of Helsinki and national ethics guidelines. The study was approved by the Danish National Committee on Health Ethics, the Data Protection Agency, and the Institutional Review Board.

Due to the notable presentation of the two brothers with isolated severe neutropenia and myelokathexis combined with the family pedigree, an autosomal recessive IEI with neutropenia was suspected. Genetic analysis by whole exome sequencing (WES) revealed that P2 was homozygous for a *CXCR2* missense variant c.865C>T, resulting in substitution of a positively charged arginine to neutral cysteine amino acid (p.R289C) (Figure 1C). P1 was found to be homozygous for the same variant by Sanger sequencing, whereas both parents and the third brother were heterozygous carriers of the variant (Figure 1D; *Online Supplementary Figure S1D*). The variant was classified as likely pathogenic according to the American College of Medical Genetics and Genomics (ACMG)/Association for Molecular Pathology (AMP) sequence variant guidance[13] (for details see *Online Supplementary Figure S1E*). The *CXCR2* R289C missense variant is rare, has a relatively high combined annotation-dependent depletion (CADD) score of 23.5 and shows a high degree of evolutionary conservation (Figure 1C, E). No individuals homozygous for the specific *CXCR2* c.865C>T variant have been reported in GnomAD v.4.1.0,[5-7] whereas heterozygosity for this variant has been associated with reduced neutrophil counts.[5] According to protein structure analysis[14] CXCR2 Arg289 is located towards the extracellular end of the seventh transmembrane α helix (Figure 1F).

To investigate the deleteriousness of the *CXCR2* patient variant, we used HeLa cells as a model. Transfected HeLa cells expressing either *CXCR2* wild-type (WT) or R289C showed that the patient variant led to reduced CXCR2 protein expression in the cytosol as well as at the cell surface (Figure 2A, B). Furthermore, the *CXCR2* R289C variant failed to mediate phosphorylation of the MAPK signaling kinase Erk1/2 in response to IL-8 stimulation, revealing impaired signaling (Figure 2C, D). Treating transfected HeLa cells with the proteasome inhibitor MG132 selectively increased the abundance of CXCR2 R289C protein and not *CXCR2*

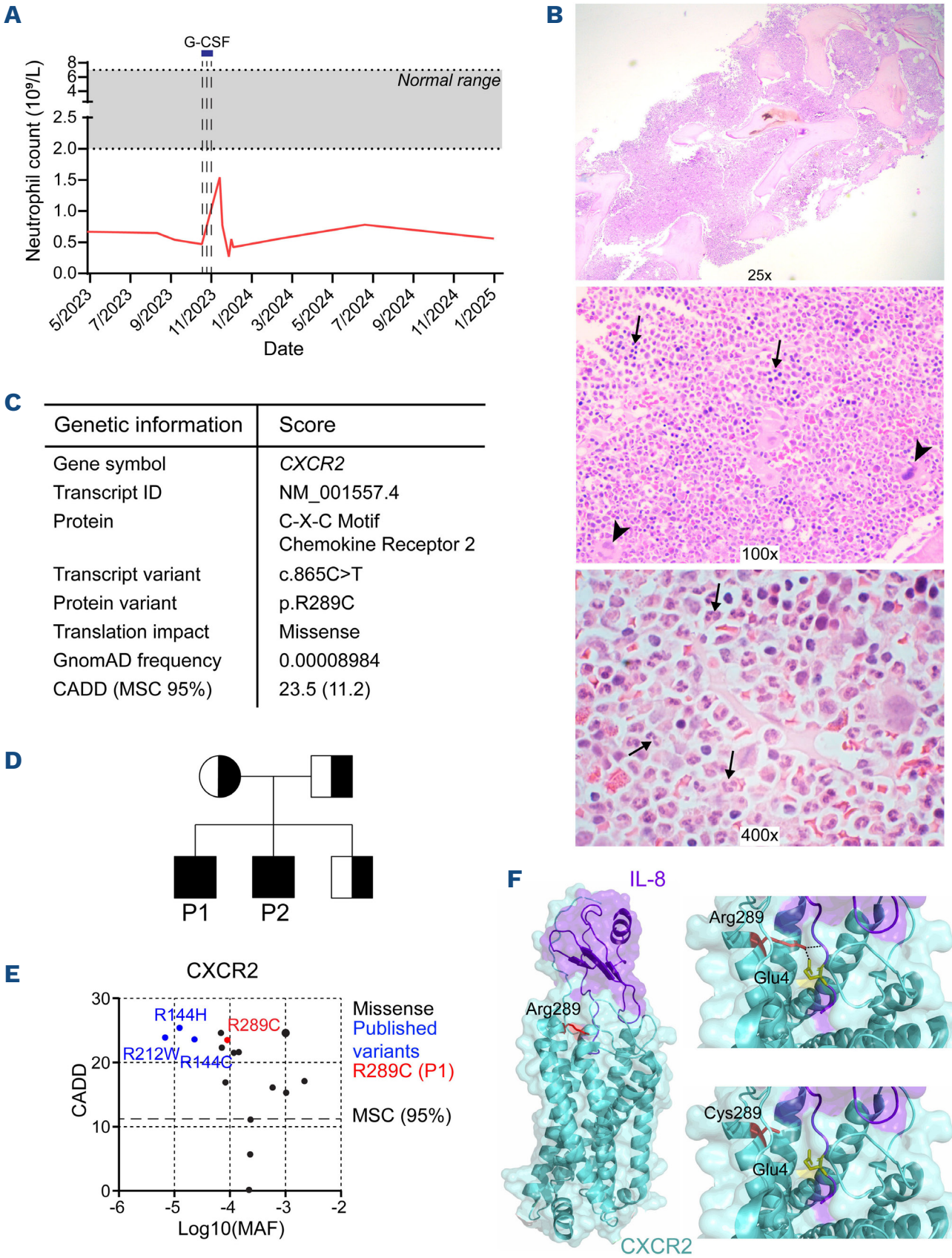

Figure 1. Identification of a Norwegian family with CXCR2 deficiency in two brothers due to homozygosity for a novel *CXCR2* variant. (A) Blood neutrophil counts for patient 1 (P1) in the period from 2023-2025. (B) Photomicrographs from bone marrow trephine biopsy of P2 taken at age 16. Top panel: 25x magnification showing hypercellular marrow with no fat cells present. Middle panel: 100x magnification showing small scattered erythroid islands (arrows) and few megakaryocytes (arrowheads) while right-shifted myelopoiesis predominates. Bottom panel: 400x magnification demonstrating numerous hypersegmented granulocytes with conspicuous thin strands of chromatin connecting nuclear lobes (arrows). (C) Summary of genetic information and *in silico* predictions for the identified *CXCR2* c.865C>T variant (p.R289C). The *CXCR2* R289C variant was identified through whole exome sequencing analysis performed on genomic DNA extracted from EDTA blood samples of the patients using a QIAsymphony instrument with corresponding DNA purification kits (Qiagen). The combined annotation-dependent depletion (CADD) score and allele frequency for *CXCR2* were found on gnomAD v4.1.0, variant 2-218135666-C-T (GRCh38). The results from a genome wide single nucleotide polymorphism array showed that P1 had a small region of homozygosity (ROH) surrounding the *CXCR2* locus on chromosome 2q35, confirming true homozygosity for the c.865C>T T variant and ruling out a large deletion. (D) Family pedigree. (E) PopViz plot for known homozygous variants reported for *CXCR2* in gnomAD v4.1.0, in this publication, or in the literature.[6,7] To ensure that all registered variants were included, we selected predicted loss-of-function and missense/in frame insertions/deletions variants for *CXCR2* in gnomAD v4.1.0. (F) Structural representation of CXCR2 in complex with monomeric interleukin 8 (IL-8), created using the cryoelectron microscopy-solved protein structure (pdb ID: 6LFO)[14] and PyMol™ v2.2.2 (Schrödinger). Left: overview with CXCR2 in cyan, IL-8 in deep purple, and amino acid Arg289 position indicated in red. Upper right: close-up view of Arg289 showing hydrogen bonds to Glu4 and polypeptide backbone of IL-8. Lower right: close-up view of Cys289. MAF: minor allele frequency; MSC: mutation significance cutoff.

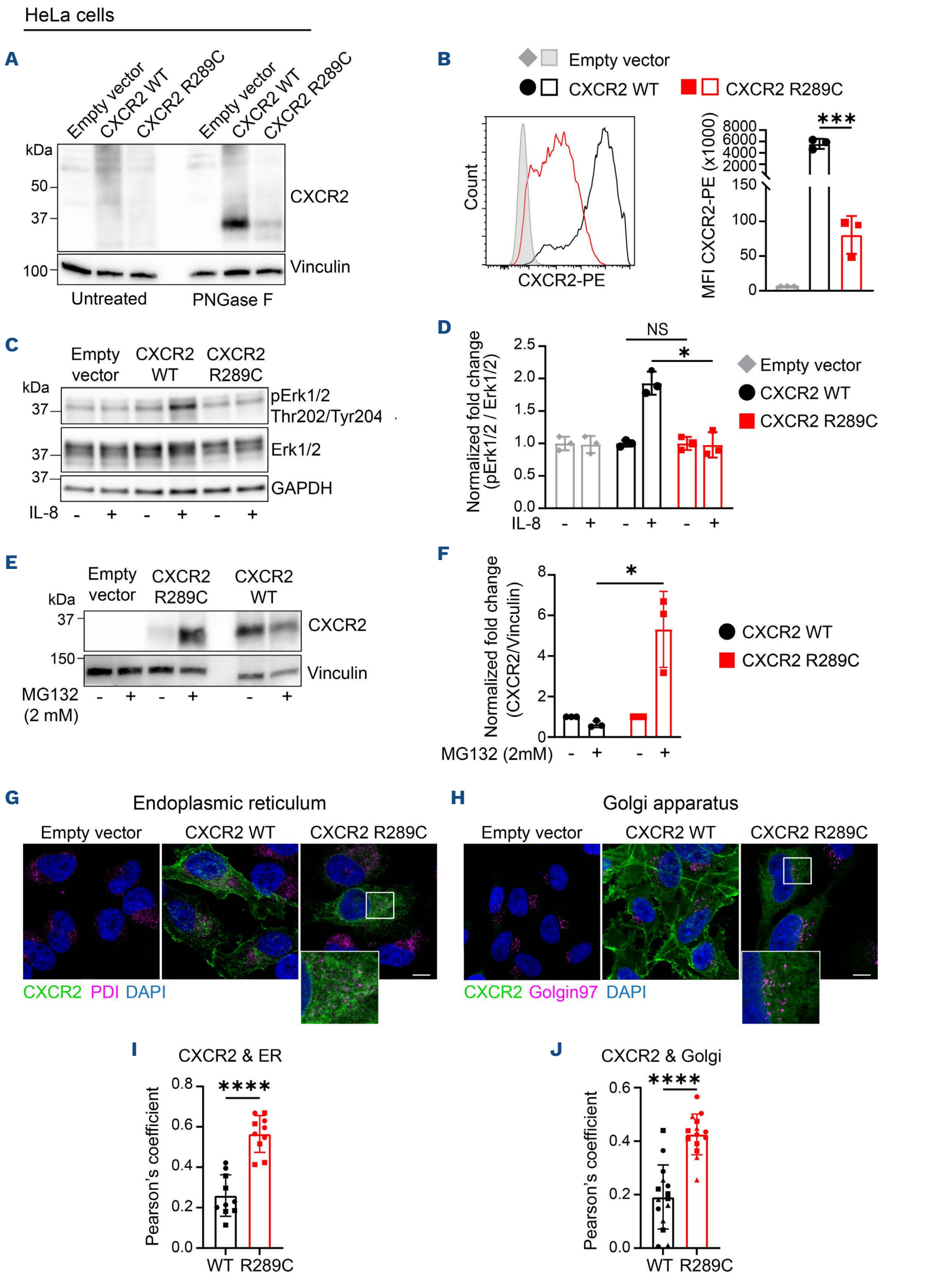

Figure 2. The patient *CXCR2* variant causes loss of CXCR2 surface expression and signaling. HeLa cells were transfected with pcDNA3.1 vectors encoding either *CXCR2* wild-type (WT), *CXCR2* R289C variant, or empty vector as negative control. (A, B) CXCR2 expression 3 days post transfection analyzed in whole-cell lysates using immunoblotting (A) and on the cell surface using flow cytometry (B). To visualize CXCR2 protein, cell lysates were treated with PNGaseF to remove N-linked glycosylation. (C, D) Two days post transfection, HeLa cells were stimulated with interleukin 8 (IL-8) (100 ng/mL) for 2 minutes. Phosphorylated Erk1/2 relative to total Erk1/2 was an-

Continued on following page.

alyzed by immunoblotting from whole-cell lysates. Shown are one representative blot (C) and quantification of 3 replicates in 2 independent experiments (D), represented as fold increase of mock-treated samples (medium only). (E, F) Twenty-four hours post transfection, HeLa cells were treated with 2 μM proteasome inhibitor MG132 or dimethyl sulfoxide (DMSO) as vehicle control for 20 hours before immunoblot analysis of CXCR2 protein and GAPDH as control. (E) Immunoblots. Lysates were treated with PNGase F before loading. (F) Quantification of (E) and 2 replicate experiments. Shown are fold increase of mock-treated samples (only medium). (G, H) Two days post transfection, HeLa cells were immunostained and analyzed by using an LSM800 confocal microscope. Shown are immunofluorescence images of transfected HeLa cells stained for CXCR2 (green), DNA (DAPI, blue), and endoplasmatic reticulum (ER) (PDI, magenta) (G) or Golgi (golgin97, magenta) (H). The scale bar (white) indicates 10 μm. (I, J) Co-localization of CXCR2 with ER (I) or Golgi (J), quantified with Pearson's correlation coefficients. Data are representative of 2 (C, D, G, I) or 3 (A, B, F, H, J) independent experiments. Graphs show individual values plus mean ± standard deviation. *P<0.05; ***P<0.001; ****P<0.0001; not significant (NS), unpaired two-tailed t test (B, I, J) and paired two-tailed t test with Holm- Šídák multiple comparisons (D, F).

WT, (Figure 2E, F) suggesting that CXCR2 R289C undergoes accelerated degradation by the proteasome pathway, thereby accounting for the reduced levels of *CXCR2* variant expression. Next, we performed confocal microscopy to visualize CXCR2 in relation to the endoplasmatic reticulum (ER) and Golgi in transfected HeLa cells. While *CXCR2* WT was expressed at high levels and with even distribution on the cell surface, the *CXCR2* R289C variant was largely undetectable at the cell surface but localized intracellularly in a perinuclear distribution. Furthermore, we observed that a significantly increased fraction of CXCR2 R289C was co-localized with both the ER and Golgi apparatus when compared to CXCR2 WT protein (Figure 2G-J; *Online Supplementary Figure S2A, B*). These data suggest a post-transcriptional defect impairing synthesis and trafficking of the *CXCR2* R289C variant through the secretory pathway, ultimately abolishing the expression of a functional CXCR2 receptor protein at the cell surface.

Having established the impaired function of the *CXCR2* R289C variant we examined patient blood cells. In patient PBMC, expression of *CXCR2* mRNA was comparable to healthy controls, whereas levels of CXCR2 protein were reduced (Figure 3A-C). Flow cytometry demonstrated that CXCR2 surface expression was significantly reduced on patient NK cells, monocytes, and neutrophils compared to controls (Figure 3D-G; *Online Supplementary Figure S2C, D*). A trans-well migration assay using whole blood revealed markedly reduced ability of patient neutrophils to migrate towards IL-8 (Figure 3H). Finally, to explore the therapeutic potential of gene correction, we used CRISPR/Cas9 gene editing with DNA templates for homology directed repair (HDR) to correct the deleterious *CXCR2* gene variant in patient PBMC. We expanded T cells from patient PBMC and performed gene editing on these cells (Figure 3I). This led to almost 100% editing efficiency for correction of the *CXCR2* c.865C>T gene variant in patient cells (Figure 3J). CRISPR activation (CRISPRa) a was used to induce CXCR2 transcription which resulted in similarly increased levels of CXCR2 surface expression in gene-edited patient and healthy control T cells (Figure 3K-L; *Online Supplementary Figure S2E*). These results confirm that the CXCR2 defect caused by the R289C variant can be corrected via gene editing to reconstitute expression of CXCR2 WT. Importantly, these data demonstrate the feasibility of this editing approach and imply a therapeutic potential for CRISPR/Cas9 gene editing for the two patients with CXCR2 deficiency, and in general for patients with this condition. The clinical presentation of these patients with a novel *CXCR2* R289C missense variant, including isolated neutropenia and myelokathexis with moderate susceptibility to infection, is largely in line with the previously published cases on CXCR2 deficiency.[5-7] Although we initially hypothesized that the CXCR2 R289C variant might interrupt IL-8 binding to the CXCR2 receptor, we instead established the mechanism to be failure of the variant to be expressed at the cell surface, likely accounting for the defective signaling and impaired chemotaxis of patient cells. At the molecular level this may be due to improper protein folding in the ER and impaired trafficking through the secretory pathway to the cell surface, combined with increased protein turnover via proteasomal degradation in the cytosol. In contrast to our findings of reduced CXCR2 surface expression on neutrophils, monocytes and NK cells,[6] Marin-Esteban *et al*. presented a case in which the R289C variant in heterozygosity did not lead to a reduced CXCR2 surface expression, suggesting that homozygosity is required for this variant to result in loss of surface expression.

CXCR2 deficiency was first described by Auer *et al*. reporting on a homozygous variant in two siblings (*CXCR2* c.968del/p.His323LeufsTer7) who suffered from congenital myelokathexis and neutropenia with recurrent bacterial infections.[5] Another publication reported four patients with different *CXCR2* variants, including a homozygous deletion on chromosome 2q35 affecting the entire *CXCR2* locus, homozygous missense variants (p.Arg144Cys and p.Ala212Trp) and compound heterozygosity for the nonsense variant p.Arg184Ter and the variant we describe herein (p.Arg289Cys)[6] (*Online Supplementary Table S1*). All four had severe oral lesions, and two responded well to G-CSF-treatment, but only the patient carrying the whole-gene deletion had myelokathexis, underscoring the variability of CXCR2 deficiency severity.[6] Finally, three additional families with CXCR2 deficiency were recently described.[7] The missense variant pArg144His was present in all three families, either in homozygous or compound heterozygous combination. In cases where bone marrow investigation was performed, a hypercellular myeloid series but no overt myelokathexis was described. The clinical phenotype was characterized by recurrent upper airway and skin infections together with oral ulcerations.

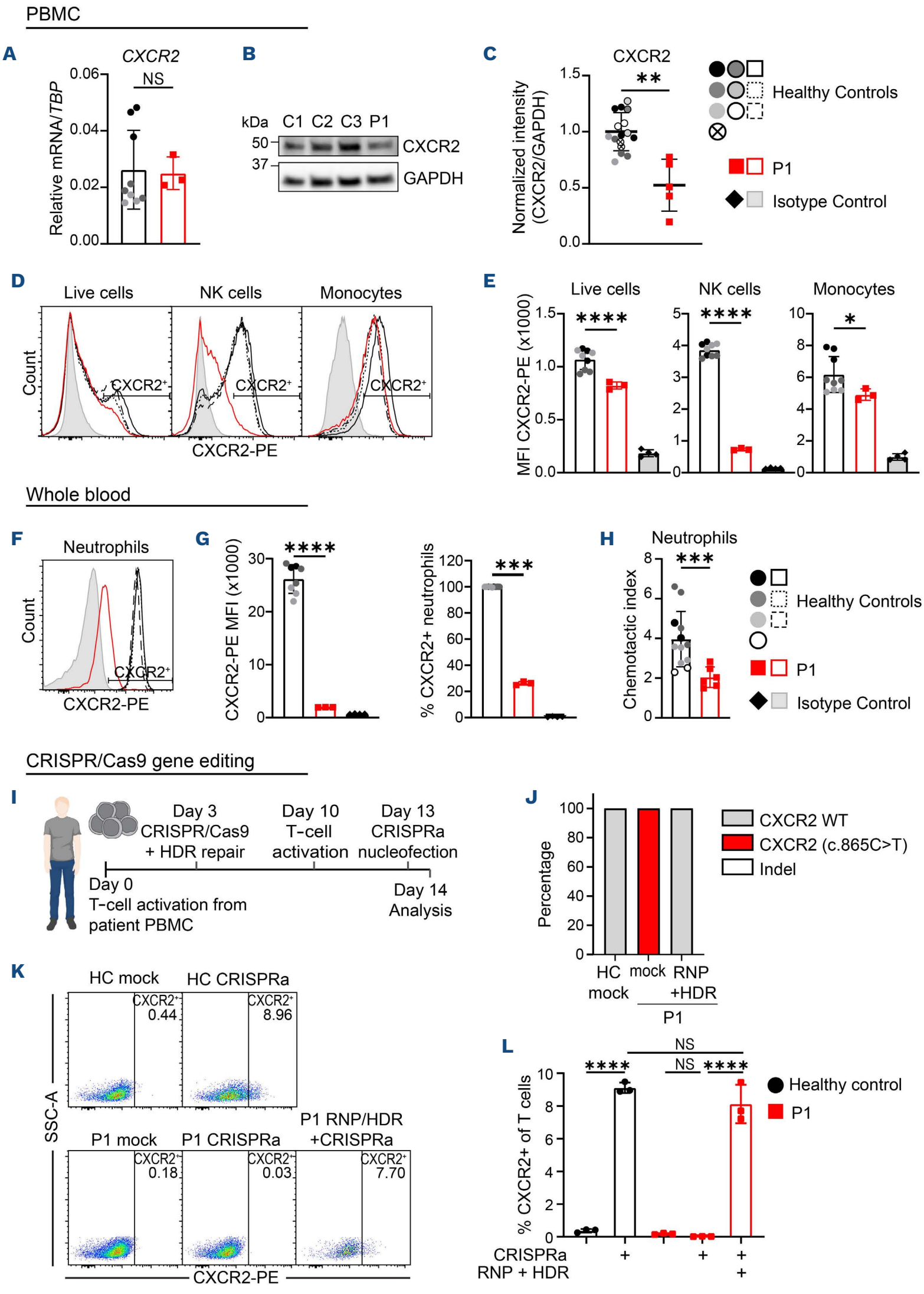

Figure 3. Patient peripheral blood mononuclear cells have impaired CXCR2 surface expression and chemotaxis and gene editing by CRISPR/Cas9-based homology-directed repair restores CXCR2 surface expression. (A, B) Determination of P1 *CXCR2* mRNA transcripts relative to *TBP* by real-time quantitative polymerase chain reaction (A, N=3 healthy controls) or P1 CXCR2 protein expression relative to GAPDH by immunoblotting (B). (C) Quantification of (B) and 4 additional replicates (N=7 healthy controls). (D, E) Histograms

Continued on following page.

of CXCR2 protein surface expression analyzed by flow cytometry on live cells, natural killer (NK) cells (CD3-CD19-CD56$^+$), and monocytes (CD14$^+$) from peripheral blood mononuclear cells (PBMC) from P1 and controls (N=3), quantified in E. (F, G) Histogram of CXCR2 protein surface expression on neutrophils (CD45$^+$CD14^{lo}CD16^{hi}) from whole blood from P1 and controls (N=3), quantified in (G.) (H) Migration of neutrophils from whole blood towards an interleukin 8 (Il-8) gradient in a Boyden-chamber, using 6 mm trans-well chambers with 3 µm pore membranes. The chemotactic index was calculated as fold increase in the number of cells migrating to IL-8 compared to the number of cells migrating to medium alone. (I) T cells were expanded from PBMC using anti-CD3/anti-CD28 activation beads 3 days before gene editing. CRISPR associated protein 9 (Cas9) ribonucleoprotein (RNP) complexes were assembled by incubating recombinant Cas9 protein and single guide RNA at a molar ratio of 1:2.5 at 25°C for 15 minutes. T cells were combined with the resulting CRISPR/Cas9 RNP, ssODN DNA template for homology-directed repair (HDR), and AZD7648 HDR enhancer, and nucleofected for CXCR2 editing. On day 10, T cells were reactivated. On day 13, *CXCR2* transcription was induced using CRISPR activation (CRISPRa). (J) Gene editing efficiency of *CXCR2* in PBMC from P1. Data show the median of 3 technical triplicates for 1 donor per group. (K, L) CXCR2 expression on gene-edited patient PBMC compared to unedited patient and healthy control PBMC, analyzed on day 14, with quantification in (L). Shown are individual values plus mean ± standard deviation. Data are representative of 1 (I-K), 2 (D-H), 3 (A) or 5 (B, C) independent experiments. Each healthy control is shown in a distinct color. **P*<0.05; ***P*<0.01; ****P*<0.001;*****P*<0.0001; not significant (NS), unpaired two-tailed *t* test with Welch's correction (A, C, E, G, H) or one-way ANOVA with Šídák's multiple comparisons test (L). Gating strategies for D-H and K are shown in *Online Supplementary Figure S2C-E*.

Overall, the currently published cases of CXCR2 deficiency reveal some variability regarding the degree of neutropenia, the extent of myelokathexis, abnormalities in IgG, IgM, and/or IgA levels, and the severity of the infectious phenotype. Indeed, myelokathexis is a rare feature among individuals with CXCR2 deficiency and was reported in only two of nine published cases, of which one was only partial (35%)[5-7] (*Online Supplementary Table S1*). Collectively, neutropenia and oral ulcerations are key features and common characteristics of CXCR2 deficiency, prompting the suggestion that CXCR2 deficiency be regarded as a genetic etiology of severe neutropenia that may or may not be associated with myelokathexis and thus distinct from WHIM syndrome. Moreover, our results together with other reports suggest *CXCR2* R289C heterozygosity as a potential risk factor for neutropenia. Whether patients with *CXCR2* deficiency may experience an increased risk of malignancy, like the case for WHIM syndrome, remains undetermined.

Treatment options for WHIM syndrome and CXCR2 deficiency are limited. Granulocyte colony- stimulating factor (G-CSF) is commonly used to treat neutropenia since it drives neutrophil differentiation and neutrophil mobilization.[15] Another treatment approach consists of the CXCR4 antagonists plerixafor[16] and mavorixafor,[17] which block CXCL12-binding to CXCR4 and thereby counteract the inhibition of neutrophil efflux from the bone marrow. Finally, we here demonstrate efficient HDR CRISPR/Cas correction of CXCR2 in patient PBMC, suggesting that a similar strategy in patient CD34$^+$ hematopoietic stem cells may constitute a curative gene therapy for these patients following further validation of efficiency and safety. To our knowledge this is the first *in vitro* attempt at demonstrating CRISPR/Cas gene correction in CXCR2 deficiency.

Authors

Daniëla M. Hinke,[1-3] Sofie R. Dorset,[1] Eirik Bratland,[4] Jonas H. Wolff,[1,3] Astrid M. Olsnes,[5,6] Jacob Giehm Mikkelsen,[1,3] Lars Helgeland,[7] Rasmus O. Bak,[1] Andreas Benneche[4] and Trine H. Mogensen[1-3]

[1]Department of Biomedicine, Aarhus University, Aarhus, Denmark; [2]Department of Infectious Diseases, Aarhus University Hospital, Aarhus, Denmark; [3]Center for Immunology of Viral infections (CIVIA), Aarhus University, Aarhus, Denmark; [4]Department of Medical Genetics, Haukeland University Hospital, Bergen, Norway; [5]Department of Clinical Science, University of Bergen, Norway; [6]Department of Hematology, Department of Medicine, Haukeland University Hospital, Bergen, Norway and [7]Department of Pathology, Haukeland University Hospital, Bergen, Norway

Correspondence:
T. H. MOGENSEN - Trine.mogensen@biomed.au.dk

https://doi.org/10.3324/haematol.2025.288111

Received: May 7, 2025.
Accepted: August 19, 2025.s
Early view: August 28, 2025.

Disclosures

No conflicts of interest to disclose.

Contributions

THM and AB conceived the idea and discussed the patient clinical history and genetic and immunological evaluation. AB and EB performed genetic analysis and identified and described the CXCR2 variant. EB performed structural analysis of the CXCR2 variant and contributed with molecular and structural biology input. LH did the histopathology of the bone marrow and described and quantified the myelokathexis. ROB and SRD designed the CRISPR strategy. DMH, SRD, and JHW performed experiments and analyzed the data together with THM, ROB, and JGM. AMO and THM cared for the patients. THM, AB, and DMH wrote the first draft of the manuscript, and all authors read, corrected and approved the final version of the manuscript.

Acknowledgments

We warmly thank the family for participating in the study. In

addition, we thank technician Bettina Bundgaard for excellent technical assistance. Flow cytometry was performed at the FACS Core Facility, Aarhus University, Denmark. Confocal imaging was performed at the Bioimaging Core Facility, Health, Aarhus University, Denmark.

Funding

THM is supported by the Independent Research Fund Denmark (0134-00006B), the Novo Nordisk Foundation (NNF21OC0067157; NNF20OC0064890), the Lundbeck Foundation (R268-2016-3927), the Innovation Fund Denmark (PASCAL-MID, 8056-00010B), the HORIZON-HLTH-2021-DISEASE-04 program under grant agreement 101057100 (UNDINE), the Danish National Research Foundation under the grant agreement DNRF164 (CiViA). DMH received funding from Innovation Fund Denmark (PASCAL-MID, 8056-00010B), and the HORIZON-HLTH-2021-DISEASE-04 program under grant agreement 101057100 (UNDINE). ROB and JGM received funding from Innovation Fund Denmark (PASCAL-MID, 8056-00010B). DMH was supported by AP Møller Foundation for the Advancement of Medical research (2024-00880) and the Aase and Ejnar Danielsens Fund for Medical Research (24-10-0515).

Data-sharing statement

Original data and protocols are available upon request from the corresponding author.

References

1. Zuelzer WW, Evans RK, Goodman J. Myelokathexis - A new form of chronic granulocytopenia. N Engl J Med. 1964;270(14):699-704.
2. Krill Carl E, Smith Hugo D, Mauer Alvin M. Chronic idiopathic granulocytopenia. N Engl J Med. 1964;270(19):973-979.
3. Wetzler M, Talpaz M, Kleinerman ES, et al. A new familial immunodeficiency disorder characterized by severe neutropenia, a defective marrow release mechanism, and hypogammaglobulinemia. Am J Med. 1990;89(5):663-672.
4. Heusinkveld LE, Majumdar S, Gao JL, McDermott DH, Murphy PM. WHIM syndrome: from pathogenesis towards personalized medicine and cure. J Clin Immunol. 2019;39(6):532-556.
5. Auer PL, Teumer A, Schick U, et al. Rare and low-frequency coding variants in CXCR2 and other genes are associated with hematological traits. Nat Genet. 2014;46(6):629-634.
6. Marin-Esteban V, Youn J, Beaupain B, et al. Biallelic CXCR2 loss-of-function mutations define a distinct congenital neutropenia entity. Haematologica. 2021;107(3):765-769.
7. Klimiankou M, Tesakov I, Tsaknakis G, et al. Expanding the genetic landscape of congenital neutropenia: CXCR2 mutations in three families revealed through whole exome sequencing. Haematologica. 2024;109(12):4140-4144.
8. Burdon PCE, Martin C, Rankin SM. Migration across the sinusoidal endothelium regulates neutrophil mobilization in response to ELR + CXC chemokines. Br J Haematol. 2008;142(1):100-108.
9. Eash KJ, Greenbaum AM, Gopalan PK, Link DC. CXCR2 and CXCR4 antagonistically regulate neutrophil trafficking from murine bone marrow. J Clin Invest. 2010;120(7):2423-2431.
10. Baggiolini M. Chemokines in pathology and medicine. J Intern Med. 2001;250(2):91-104.
11. The human protein atlas: CXCR2 - single cell types. Available from v24.0 proteinatlas.org. URL: https://www.proteinatlas.org/ENSG00000180871-CXCR2/single+cell+type. Accessed March 22, 2025.
12. Karlsson M, Zhang C, Méar L, et al. A single-cell type transcriptomics map of human tissues. Sci Adv. 2021;7(31):eabh2169.
13. Richards S, Aziz N, Bale S, et al. Standards and guidelines for the interpretation of sequence variants: a joint consensus recommendation of the American College of Medical Genetics and Genomics and the Association for Molecular Pathology. Genet Med. 2015;17(5):405-424.
14. Liu K, Wu L, Yuan S, et al. Structural basis of CXC chemokine receptor 2 activation and signalling. Nature. 2020;585(7823):135-140.
15. Mehta HM, Malandra M, Corey SJ. G-CSF and GM-CSF in neutropenia. J Immunol. 2015;195(4):1341-1349.
16. McDermott DH, Pastrana DV, Calvo KR, et al. Plerixafor for the treatment of WHIM syndrome. N Engl J Med. 2019;380(2):163-170.
17. Dale DC, Firkin F, Bolyard AA, et al. Results of a phase 2 trial of an oral CXCR4 antagonist, mavorixafor, for treatment of WHIM syndrome. Blood. 2020;136(26):2994-3003.